Multidimensional quasiperiodic antiphase dynamics

A. G. Vladimirov
Physics Faculty, St. Petersburg State University, 198904 St. Petersburg, Russia

E. A. Viktorov
Institute for Laser Physics, 199034 St. Petersburg, Russia

Paul Mandel
Optique Nonlinéaire Théorique, Université Libre de Bruxelles, Campus Plaine Code Postal 231, B-1050 Bruxelles, Belgium
(Received 12 April 1999)

We study analytically the $(N-1)$-fold degenerate Hopf bifurcation at which N stationary modes with identical parameters become unstable in a model of a solid-state laser with intracavity second harmonic generation. We use the normal form method and exploit the symmetries of the problem. Up to $N=3$, stable periodic antiphased solutions emerge from the Hopf bifurcation. For $N=4$, stable quasiperiodic solutions arise from the degenerate Hopf bifurcation. For $N>4$, the quasiperiodic solutions may be unstable. Then chaotic itineracy is observed numerically close to the degenerate Hopf bifurcation. [S1063-651X(99)07808-3]

PACS number(s): 05.45.Xt, 05.40.−a, 42.65.Ky

I. INTRODUCTION

Antiphase oscillations were studied theoretically and experimentally in coupled Josephson junctions [1,2], coupled chemical oscillators [3], olfactory systems [4], multimode lasers [5–15], and coupled laser arrays [16]. In a solid-state laser with intracavity second harmonic generation (ISHG) operating on N longitudinal modes, this type of oscillations can appear after a Hopf bifurcation of the cw regime characterized by an equal intensity of all the modes. When all the excited modes belong to the same electric field polarization and have equal gains, losses, and cross-saturation coefficients, this bifurcation is degenerate and produces different kinds of antiphase states. In particular, there is a periodic solution in which all modes oscillate with the same wave form but each mode has its phase shifted by $2\pi/N$ from the previous mode. Permutation among the modes produces $(N-1)!$ such states. These solutions have been referred to as type-1 antiphase dynamics (AD1) in the ISHG problem [10,11]. They have also been called splay-phase states [16,17] or ponies on a merry-go-round [18]. AD1 solutions are similar to the traveling (rotating) wave solutions described in a ring of coupled oscillators [16,19,20]. Due to their high multiplicity, the AD1 solutions have potential applications as basic elements of rewritable dynamic pattern memory [21]. Although these solutions are most commonly found in the context of laser antiphase dynamics, their stability properties for the ISHG model have never been studied systematically. This paper is an attempt to fill this gap. For that purpose, we derive the normal form equations governing the evolution of the laser modal intensities near the Hopf instability threshold. Using these equations we analyze the stability properties of the AD1 solutions oscillating on an arbitrary number of modes. We show that for the model we study, near the degenerate Hopf bifurcation point the periodic AD1 solutions are unstable if $N>3$. Stable AD1 regimes can appear only at a finite distance from the degenerate bifurcation point if the mode number N is small enough. We describe the instabilities of the AD1 solution leading to quasiperiodic antiphase states. Though the validity of our analytical results is limited to a small vicinity of the degenerate Hopf bifurcation point, qualitative results concerning the antiphased properties of these quasiperiodic solutions turn out to be in a good agreement with those obtained by numerical integration of the original laser equations in a wide parameter domain.

This paper is organized as follows. After this introduction, we present the model for ISHG lasers in Sec. II. In Sec. III, we introduce the general formalism for the analysis of the degenerate Hopf bifurcation of the N-mode solution based on symmetry considerations. The main section is Sec. IV where the explicit normal form is derived from the physical equations. In Sec. V, the general analysis is applied to the three-mode regime, the only regime for which stable periodic AD1 solutions emerge though the Hopf bifurcation is degenerate. Section VI deals with the four-mode regime in which the Hopf bifurcation leads to stable quasiperiodic solutions. In Sec. VII we derive some properties of the bifurcating solution for five and more oscillating modes. The results are summarized and discussed in the conclusion.

II. MODEL EQUATIONS

A frequency-doubled solid-state laser can be described by the equations [22]

$$\eta \frac{dI_k}{dt} = I_k\left[G_k - \alpha + \varepsilon I_k - 2\varepsilon \sum_{r=1}^{N} I_r \right], \tag{1}$$

$$\frac{dG_k}{dt} = \gamma - G_k\left[1 + (1-\beta) I_k + \beta \sum_{r=1}^{N} I_r \right]. \tag{2}$$

Here I_k (G_k) is the intensity (gain) of the mode k. The parameter η is defined as $\eta = \tau_c/\tau_f$ where τ_c and τ_f are the cavity round-trip and fluorescence lifetime, respectively. The cavity loss parameter is α, the linear gain is γ, and β is the

cross-saturation parameter. These three parameters are assumed to be the same for all the modes. N is the total number of laser modes. We assume that all modes have the same electric field polarization. The parameter ε describes the nonlinear losses due to the frequency doubling process in the KTP (KTiOPO) crystal. Note that all modes are strictly equivalent since they have exactly the same parameters. Therefore Eqs. (1) and (2) are $\mathbf{S}_N$ equivariant, where $\mathbf{S}_N$ is the symmetry group consisting of all possible permutations of modal indices.

III. DEGENERATE HOPF BIFURCATION

It has been shown that for $\varepsilon, \eta \ll 1$ and γ small enough, the only stable steady-state solution of Eqs. (1) and (2) is that for which all N lasing modes have equal intensities and equal gains [9]

$$I_j = I > 0, \quad G_j = G > 0, \quad j = 1, \ldots, N. \tag{3}$$

Increasing the pump parameter, this solution undergoes a Hopf bifurcation leading to antiphase oscillations of the modal intensities. The Hopf bifurcation condition is [9]

$$\gamma = \frac{I_0}{\theta}[\alpha + \varepsilon I_0(2N-1)], \quad I_0 = \frac{\theta}{1-\theta[1+(N-1)\beta]}, \tag{4}$$

where I_0 is the critical modal intensity and $\theta = \eta/\varepsilon$. At the bifurcation boundary (4) the linear stability analysis of the solution (3) yields $N-1$ identical pairs of pure imaginary eigenvalues. Hence, for $N>2$ the condition (4) defines a *degenerate* Hopf bifurcation (hereafter referred to as $\mathcal{H}$) that cannot be described by means of the usual Hopf bifurcation formalism. The degeneracy of the Hopf bifurcation results from the symmetries imposed by the equivalence of the laser modal parameters. Unlike a nondegenerate Hopf bifurcation which produces only a single branch of periodic solutions, the number of solutions bifurcating from the N-mode solution at $\mathcal{H}$ increases with increasing N. Among these solutions are the $(N-1)!$ AD1 antiphased periodic solutions for which all N modes oscillate with the same wave form but with the phase shifted by $2\pi/N$ from another mode [1]. However, we show in the next sections that more solutions can exist, in particular, stable quasiperiodic antiphased solutions.

IV. NORMAL FORM EQUATIONS

A. Linear transformation

Consider the Hopf bifurcation point defined by Eq. (4). As already mentioned, for $N>2$ Eqs. (4) correspond to a degenerate bifurcation. After introducing the variables

$$x_{2j-1} = \varepsilon(I_j - I), \quad x_{2j} = G_j - \alpha - \varepsilon I(2N-1), \quad \tau = tI/\theta,$$

where $j = 1, \ldots, N$ and I is the steady-state modal intensity (3), Eqs. (1) and (2) are transformed into

$$\partial_\tau \mathbf{x} = J\mathbf{x} + \mathbf{K}(\mathbf{x},\mathbf{x}), \tag{5}$$

where $\mathbf{x} = (x_1, x_2, \ldots, x_{2N})^T$ and $\mathbf{K}(\mathbf{x},\mathbf{x})$ is a vector whose components are homogeneous second order polynomials in the x_j. The $2N \times 2N$ Jacobian matrix J has the structure

$$\begin{pmatrix} L_1 & L_2 & \ldots & L_2 \\ L_2 & L_1 & \ldots & L_2 \\ \vdots & \vdots & \ddots & \vdots \\ L_2 & L_2 & \ldots & L_1 \end{pmatrix}, \tag{6}$$

where L_1 and L_2 are the 2×2 matrices

$$L_1 = \begin{pmatrix} -1 & 1 \\ -\chi & -1+2\rho \end{pmatrix}, \quad L_2 = \begin{pmatrix} -2 & 0 \\ -\beta\chi & 0 \end{pmatrix},$$
$$\chi = \theta\left(2N-1+\frac{\alpha}{\varepsilon I}\right), \quad \rho = \frac{\theta}{2I_0 I}(I - I_0), \tag{7}$$

and I_0 is the critical modal intensity defined by Eq. (4). The matrix L_2 results from the coupling between modes. The eigenvalues of the matrix (6) are

$$\lambda_j = \rho - i\omega, \quad \lambda_{N+j} = \lambda_j^*, \quad \lambda_N = -N + \rho - i\Omega,$$
$$\lambda_{2N} = \lambda_N^*,$$

with $j = 1, \ldots, N-1$, and

$$\omega^2 = \chi(1-\beta) - (1-\rho)^2,$$
$$\Omega^2 = \chi[1+(N-1)\beta] - (N-1+\rho)^2. \tag{8}$$

The parameter ρ is the deviation from the Hopf bifurcation point, and ω and Ω are the two relaxation oscillation frequencies [12]. The Hopf bifurcation is possible only if $\omega^2 > 0$. In the following analysis we assume that Ω^2 is also positive. The stable eigenvalues λ_N and λ_{2N} are associated with the eigenvectors belonging to the synchronization manifold $x_1 = x_3 = \cdots = x_{2N-1}$ and $x_2 = x_4 = \cdots = x_{2N}$, whereas the remaining eigenvalues are associated with the eigenvectors orthogonal to this manifold [23]. The eigenvectors $\mathbf{v}_l = \{v_{lm}\}$ ($\mathbf{w}_l = \{w_{lm}\}$) of the matrix J (transposed matrix J^T) can be chosen as

$$v_{j,2k-1} = -\frac{ie^{2\pi ij(k-1)/N}}{2N \operatorname{Im}\lambda_j},$$
$$v_{j,2k} = -(1-2\rho+\lambda_{N+j})v_{j,2k-1}, \tag{9}$$
$$w_{j,2k-1} = (1-2\rho+\lambda_j)w_{j,2k}, \quad w_{j,2k} = e^{-2\pi ij(k-1)/N}, \tag{10}$$
$$\mathbf{v}_{N+j} = \mathbf{v}_j^*, \quad \mathbf{w}_{N+j} = \mathbf{w}_j^*, \tag{11}$$

with $j,k = 1, \ldots, N$. The eigenvectors $\mathbf{v}_l$ and $\mathbf{w}_m$ are biorthogonal,

$$\sum_{p=1}^{2N} v_{lp} w_{mp} = \delta_{lm},$$

and obey the relations

$$\sum_{k=1}^{N} v_{j,2k-1} = \sum_{k=1}^{N} v_{j,2k} = \sum_{k=1}^{N} w_{j,2k-1} = \sum_{k=1}^{N} w_{j,2k} = 0, \tag{12}$$

with $j=1,\ldots,N-1$. The relations (12) are equivalent to the sum rule derived in [10,11].

We introduce the linear change of variables

$$y_j=\sum_{k=1}^{2N} w_{j,k}x_k, \quad y_{N+j}=\sum_{k=1}^{2N} w_{N+j,k}x_k=y_j^*, \qquad (13)$$

with $j=1,\ldots,N$ in Eqs. (5) which are transformed into

$$\frac{dy_j}{d\tau}=\lambda_j y_j+Y_j(y_1,\ldots,y_N,y_1^*,\ldots,y_N^*), \qquad (14)$$

where $j=1,\ldots,N$ and Y_j are homogeneous second order polynomials in y_k and y_k^*.

Since all lasing modes have identical parameters, Eqs. (1) and (2) are equivariant under any permutations of the modal indices. As a result, Eqs. (14) must also possess symmetry properties. Let us consider the transformation defined by the cyclic permutation of the modal indices

$$(1,2,3,\ldots,N)\rightarrow(N,1,2,\ldots,N-1). \qquad (15)$$

Taking into account Eqs. (13) and (10), it is easy to show that the symmetry property (15) of Eqs. (1) and (2) implies that Eqs. (14) are equivariant under the action of the cyclic group $\mathbf{Z}_N$ which is defined by

$$\zeta(y_1,\ldots,y_N)=(e^{i\zeta}y_1,\ldots,e^{iN\zeta}y_N), \quad \zeta=2\pi/N. \qquad (16)$$

Let us fix the index of the first lasing mode ($j=1$) and consider all possible permutations of the remaining $N-1$ modal indices, $j=2,\ldots,N$. It follows from Eq. (13) that each of these permutations generates a linear transformation of the variables $y_1,\ldots,y_N$. According to Eq. (10), w_{Nk} does not depend on k. Hence y_N is invariant under any mode permutation. Using the relations (9) we get the following transformation rule for the remaining $N-1$ variables:

$$\mathbf{y}\rightarrow S_n\mathbf{y}, \quad S_n=V^{-1}P_nV, \quad n=1,\ldots,(N-1)!, \qquad (17)$$

where $\mathbf{y}=(y_1,\ldots,y_{N-1})^T$. The elements of the $(N-1)\times(N-1)$ matrix $V=\{V_{lm}\}$ in Eq. (17) are $V_{lm}=e^{2\pi ilm/N}$ while $P_1,\ldots,P_{(N-1)!}$ are the unitary matrices obtained from the $(N-1)\times(N-1)$ identity matrix using all possible row permutations. The linear transformations (17) define a unitary representation of the symmetric group $\mathbf{S}_{N-1}$ consisting of all the permutations among the $N-1$ modal indices, $j=2,\ldots,N$. The symmetries of Eqs. (1) and (2) imply that the right hand side of Eqs. (14) commutes with all the transformations defined by Eq. (17). The symmetry group $\mathbf{S}_{N-1}$ has $(N-1)!$ elements, each corresponding to a unitary matrix S_n. Note, however, that the action of this group can be generated by only $N-2$ linear transformations. Every permutation of the modal indices can be obtained by the sequential application of $N-2$ permutations, each of which interchanges only two neighboring indices j and $j+1$.

There is also a transformation in Eq. (17) which corresponds to the flip symmetry of Eqs. (14) defined by

$$\kappa(y_1,y_2,\ldots,y_{N-1},y_N)=(y_{N-1},y_{N-2},\ldots,y_1,y_N). \qquad (18)$$

This symmetry corresponds to the permutation

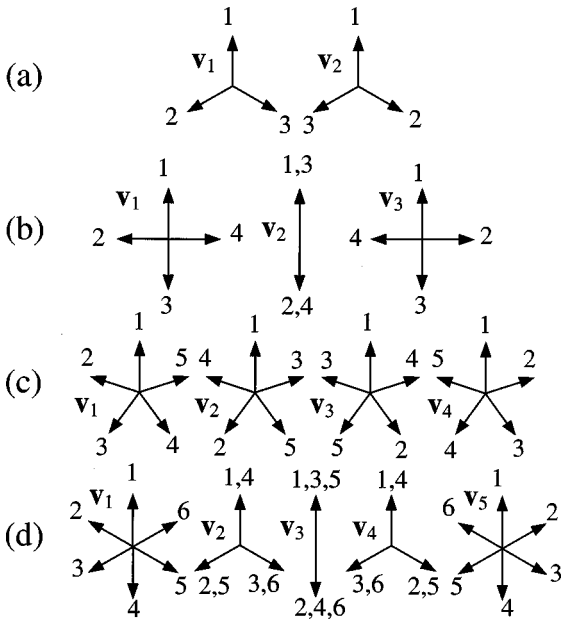

FIG. 1. Schematic representation of the eigenvectors $\mathbf{v}_1,\ldots,\mathbf{v}_{N-1}$ defined by Eqs. (9) for the case (a) $N=3$, (b) $N=4$, (c) $N=5$, and (d) $N=6$. The arrow labeled k corresponds to the modal intensity I_k. Phase shift between the oscillating modal intensities is determined by the angle between the rays. If the greatest common divisor of m and N is equal to p, the vector $\mathbf{v}_m$ is represented by a diagram having p rays.

$$(1,2,3,\ldots,N)\rightarrow(1,N,N-1,\ldots,2).$$

In the new variables (13), the sum of the mode intensities takes the form

$$\begin{aligned}\sum_{k=1}^{N} I_k(t)&=\sum_{k=1}^{N}\left(I+\frac{x_{2k-1}}{\varepsilon}\right)\\&=NI+\frac{1}{\varepsilon}\left(\sum_{k=1}^{N}\sum_{j=1}^{N} v_{j,2k-1}y_j+\text{c.c.}\right)\\&=NI-\frac{\operatorname{Im} y_N(\tau)}{\varepsilon\Omega},\end{aligned} \qquad (19)$$

where NI is the sum of the steady-state modal intensities. It follows from Eq. (19) that the time-dependent part of the total intensity is proportional to the imaginary part of the variable y_N corresponding to the eigenvalue $-N+\rho-i\Omega$. This accounts for the fact that the total intensity of the modes exhibits only one relaxation frequency, which is Ω [12]. The relation (19) also explains another peculiar feature of the total output laser intensity which appears in the course of the antiphase oscillations. Since y_N and y_N^* are the only variables associated with eigenvalues having finite negative real parts at the Hopf bifurcation point $\rho=0$ in the limit $t\rightarrow\infty$, these variables and, hence, the total output laser intensity, have much smoother behavior at least near $\mathcal{H}$ than the intensities of the individual modes [12,13], which can be expressed as linear combinations of the order parameters y_k and y_k^* with $k=1,\ldots,N-1$.

Each of the eigenvectors defined by Eqs. (9), (10), and (11) is associated with a type of antiphased regime. A sche-

matic representation of the antiphased regimes corresponding to the basis eigenvectors $\mathbf{v}_1, \ldots, \mathbf{v}_{N-1}$ is shown in Fig. 1 for $N=3$, 4, 5, and 6. Each ray in this figure depicts a laser mode, whereas the angle between the rays describes the relative phase shift between the oscillations of the modal intensities. Periodic antiphase solutions emerging from $\mathcal{H}$ can be associated with linear combinations of the basis eigenvectors (9). In particular, for $N=4$ there exist $(4-1)!=6$ types of antiphased AD1 regimes which can be obtained by mode permutations. Only two of them, those corresponding to the eigenvectors $\mathbf{v}_1$ and $\mathbf{v}_3$, are presented in Fig. 1(b). The remaining four regimes are associated with two pairs of linear combinations $[\mathbf{v}_1+(1\pm i)\mathbf{v}_2\mp i\mathbf{v}_3]/2$ and $[\mathbf{v}_3+(1\pm i)\mathbf{v}_2 \mp i\mathbf{v}_1]/2$.

The linear coordinate change (13) with w_{jk} defined by Eqs. (10) and (11) is similar to the discrete Fourier transformation which is used to study the dynamics of coupled oscillators (see, for example, [16,20,23]). Therefore, the amplitudes y_j can be considered as Fourier modes characterized by a certain wave number as shown in the next section.

B. Nonlinear analysis

Close to the Hopf bifurcation (4), we can transform Eqs. (14) into normal form equations governing the time evolution of the order parameters $y_1, \ldots, y_{N-1}$. The transformation is performed in the vicinity of the steady-state solution with the help of near identity polynomial changes of variables [24–26]. In the new variables z_j, $j=1,2,\ldots,N-1$, the resulting unfolded normal form equations take the form

$$\frac{dz_j}{d\tau}=(\rho-i\omega)z_j+\sum_{\mathbf{p},\mathbf{q}} A_{j\mathbf{pq}} z_1^{p_1}\cdots z_{N-1}^{p_{N-1}} z_1^{*q_1}\cdots z_{N-1}^{*q_{N-1}}, \tag{20}$$

where $j=1,\ldots,N-1$, $\mathbf{p}=(p_1,\ldots,p_{N-1})\geqslant\mathbf{0}$, and $\mathbf{q}=(q_1,\ldots,q_{N-1})\geqslant\mathbf{0}$. The coefficients $A_{j\mathbf{pq}}$ of the normal form depend on the parameters of the original laser equations. According to the normal form theory [24] the sum over $\mathbf{p}$ and $\mathbf{q}$ in the right hand side of Eqs. (20) contains only third and higher order resonant terms which are characterized by $\Sigma_{k=1}^{N-1}(p_k-q_k)=1$. This means that the right hand side of Eqs. (20) commutes with the $\mathbf{S}^1$ circle group action generated by the transformation

$$\vartheta(z_1,\ldots,z_{N-1})=e^{i\vartheta}(z_1,\ldots,z_{N-1}), \quad \vartheta\in\mathbf{S}^1. \tag{21}$$

This property is inherent in the Hopf bifurcation. In addition, the normal form equations (20) preserve all the symmetries of Eqs. (14). In particular, it follows from the symmetry property (16) that only the nonlinear terms which obey the relation

$$\mathrm{mod}\left(\sum_{k=1}^{N-1} k(p_k-q_k),N\right)=j \tag{22}$$

are present in the right hand side of the equation governing the evolution of the variable z_j. By definition $\mathrm{mod}(a,b)$ is the fractional part of a/b. The remaining symmetry properties (17) of Eqs. (14) imply certain relations between the normal form coefficients $A_{j\mathbf{pq}}$. With these properties taken into account, Eq. (20) truncated to retain terms up to third order becomes

$$\frac{dz_j}{d\tau}=(\rho-i\omega)z_j-2az_j\sum_{k=1}^{N-1}|z_k|^2 - bz_{N-j}^*\sum_{k=1}^{N-1} z_k z_{N-k}-c\sum_{k,l,m=1}^{N-1}\delta_{kl}^{mj} z_m^* z_k z_l, \tag{23}$$

where $j=1,\ldots,N-1$, $\delta_{kl}^{mj}=1$ for $\mathrm{mod}(k+l-m-j,N)=0$, and $\delta_{kl}^{mj}=0$ otherwise. Explicit expressions for the complex coefficients a, b, and c in terms of the parameters of Eqs. (1) and (2) are given in the Appendix.

The symmetry property (18) results in the flip symmetry

$$\kappa(z_1,z_2,\ldots,z_{N-1})=(z_{N-1},z_{N-2},\ldots,z_1) \tag{24}$$

of Eqs. (20) and (23). Together with Eq. (16), the symmetry property (24) constitutes the dihedral symmetry group $\mathbf{D}_N$. Therefore, the symmetry group of the normal form equations contains $\mathbf{D}_N$ as a subgroup.

In the following sections we analyze the stability properties of the third order normal form equations (23) in the limit

$$\eta,\varepsilon\ll 1, \quad \alpha,\beta,\theta\equiv\eta\varepsilon=O(1), \tag{25}$$

which is suggested by the experiments [5]. In the limit (25), using the asymptotic expressions for the normal form coefficients given in the Appendix, we obtain the scalings

$$\mathrm{Re}\,a,\mathrm{Re}\,c=O(1), \quad \mathrm{Im}\,a=O(\varepsilon^{-1/2}), \quad \mathrm{Re}\,b=O(\varepsilon^{-1}),$$
$$\mathrm{Im}\,b,\mathrm{Im}\,c=O(\varepsilon^{-3/2}), \tag{26}$$

$$\mathrm{Re}\,a,\mathrm{Re}\,b>0, \quad \mathrm{Re}\,c,\mathrm{Im}\,a,\mathrm{Im}\,c<0. \tag{27}$$

If $N\to\infty$ the normal form equations (23) can be written as

$$\partial_\tau W=(\rho-i\omega)W-2aW\int_{-1/2}^{1/2}|W|^2\,d\xi - bW^*\int_{-1/2}^{1/2}W^2\,d\xi-cW|W|^2, \tag{28}$$

with a periodic boundary condition $W(\tau,-1/2)=W(\tau,1/2)$, where ξ is the continuous analog of the discrete variable $j/N-1/2$. For even N, substituting $W(\tau,\xi)=\Sigma_{j=1}^{N-1}z_j(\tau)e^{2\pi i(j-N/2)\xi}$ into Eq. (28) we get the normal form equations (23) which govern the time evolution of the Fourier modes z_j. Hence, the Fourier mode z_j can be associated with the wave number $K_j=j-N/2$. In Eq. (28) the terms proportional to a and b describe the global coupling. In the absence of coupling ($a=b=0$) the Hopf bifurcation is subcritical if $\mathrm{Re}\,c<0$. As will be shown later, this inequality leads to the instability of the periodic AD1 solutions in a laser with mode number $N>3$.

According to the scalings (26), the real parts of the normal form coefficients can be neglected to leading order in ε. Then, Eqs. (23) at $\rho=0$ become conservative with an energy integral defined by $E_0=\Sigma_{k=1}^{N-1}|z_k|^2$. The corresponding integral of Eq. (28) is $E_0=\int_{-1/2}^{1/2}|W|^2\,d\xi$. This result is

in agreement with a more general result valid not only in the vicinity of the instability threshold [27]. In the conservative limit the third order normal form (23) has an additional integral defined by $E_1=\mathrm{Im}\, b|\Sigma_{k=1}^{N-1} z_k z_{N-k}|^2 + \mathrm{Im}\, c\Sigma_{j,k,l,m=1}^{N-1}\delta_{kl}^{mj} z_j^* z_m^* z_k z_l$ in the discrete case and $E_1 = \mathrm{Im}\, b|\int_{-1/2}^{1/2} W^2\, d\xi|^2 + \mathrm{Im}\, c\int_{-1/2}^{1/2}|W|^4\, d\xi$ in the continuous case.

In order to examine the antiphase properties of the normal form equation solutions, we need to come back to the variables x_{2j-1} describing the deviations of the modal intensities from the steady-state intensity

$$\varepsilon(I_j-I)=x_{2j-1}=\sum_{k=1}^{N} v_{k,2j-1}y_k+\text{c.c.} \tag{29}$$

Any type of AD1 regime can be associated with a sequence $\{j_1,j_2,\ldots,j_N\}$, where two consecutive indices j_k and j_{k+1} correspond to modal intensities oscillating with the phase shift $2\pi/N$. Consider the solution of Eqs. (23),

$$z_1=r_1 e^{-i(\omega+\omega_1)\tau},\quad z_k=0\quad (k>1), \tag{30}$$

where ω_1 is the nonlinear frequency shift proportional to the unfolding parameter ρ. It describes the periodic AD1 regime corresponding to the temporal pattern $\{1,2,\ldots,N\}$ associated with the eigenvector $\mathbf{v}_1$. Replacing y_1 in Eq. (29) by z_1 from Eq. (30) we get the relation $x_{2j-1} \approx r_1 v_{1,2j-1} e^{-i(\omega+\omega_1)\tau}+\text{c.c.}$, where the complex functions $v_{1,2j-1}$ determine the phase shift between the oscillating modal intensities I_k and I_{k+1} which equals $2\pi/N$.

Let us suppose that the solution (30) undergoes a secondary Hopf bifurcation leading to a quasiperiodic solution. We assume that near the secondary bifurcation point the contributions of all the Fourier modes except for z_1 and z_{m+1} are negligible and the quasiperiodic solution can be written in the form

$$z_1=r_1 e^{-i(\omega+\omega_1)\tau},\quad z_{m+1}=r_{m+1}e^{-i(\omega+\omega_{m+1})\tau},$$

$$|\omega_{1,m+1}|\ll\omega,\quad r_1\gg r_{m+1}\gg|z_k|\quad (k\neq 1,m+1). \tag{31}$$

The solution (31) is characterized by two frequencies. The carrier frequency $\omega+\omega_1$ is determined by the frequency of the periodic AD1 solution (30) and the envelope frequency is equal to the frequency splitting of the variables z_1 and z_{m+1}. The temporal pattern $\{1,2,\ldots,N\}$ associated with the antiphased carrier of the quasiperiodic solution (31) is the same as for the AD1 solution (30). Replacing y_k by z_k in Eq. (29) and neglecting the contributions of all the amplitudes except for z_1 and z_{m+1}, we get for the oscillating parts of the modal intensities $x_{2j-1}\approx Z_j(\tau)v_{1,2j-1}e^{-i(\omega+\omega_1)\tau}+\text{c.c.}$ The time dependence of $Z_j(\tau)$ determines the envelope of the quasiperiodic solution (31). Using Eq. (9), $Z_j(\tau)$ can be written as

$$Z_j(\tau)=r_1+e^{2\pi i m(j-1)/N}r_{m+1}e^{-i\Delta\omega\tau}, \tag{32}$$

where $\Delta\omega=\omega_{m+1}-\omega_1$ is the frequency splitting of z_1 and z_{m+1} and $e^{2\pi i m(j-1)/N}$ describes the relative phase shift between the envelopes of the quasiperiodic modal intensities. It can be deduced from Eq. (32) that for $\Delta\omega>0$ ($\Delta\omega<0$) the low-frequency antiphased envelope of the quasiperiodic solution (31) has the temporal pattern associated with the eigenvector $\mathbf{v}_m$ ($\mathbf{v}_{N-m}$).

Similar considerations can be applied if the quasiperiodic regime (31) itself undergoes a secondary Hopf bifurcation leading to a three-dimensional (3D) torus. If such a bifurcation leads to the appearance of a third Fourier mode z_{n+1} ($n\neq m$) oscillating at frequency $\omega+\omega_{n+1}$ such that $|\Delta\omega'| = |\omega_{n+1}-\omega_1|\ll|\Delta\omega|\ll\omega$, then the resulting quasiperiodic solution will exhibit two envelopes associated with the eigenvectors $\mathbf{v}_m$ (or $\mathbf{v}_{N-m}$) and $\mathbf{v}_n$ (or $\mathbf{v}_{N-n}$). The first envelope is characterized by the frequency $|\Delta\omega|\ll\omega$, the second envelope has $|\Delta\omega'|\ll|\Delta\omega|$.

V. THREE MODES

For a laser operating with three identical modes, $\mathcal{H}$ corresponds to two identical pairs of pure imaginary eigenvalues. In this case the normal form equations are $\mathbf{D}_3\times\mathbf{S}^1$ equivariant, where $\mathbf{D}_3$ is the dihedral symmetry group which is isomorphic to the symmetry group $\mathbf{S}_3$ of the original laser equations. $\mathbf{D}_3$ is generated by

$$\zeta(z_1,z_2)=(e^{i\zeta}z_1,e^{-i\zeta}z_2),\quad \zeta=2\pi/3, \tag{33}$$

$$\kappa(z_1,z_2)=(z_2,z_1). \tag{34}$$

A detailed study of a Hopf bifurcation with $\mathbf{D}_N$ symmetry was presented in [20]. However, in our particular case, the relations (26) and (27) reduce substantially the number of possible stable solutions. For $N=3$, the normal form equations (20) limited to the fifth order take the form

$$\partial_\tau z_j = z_j[\rho - i\omega - A|z_j|^2 - B|z_k|^2 - p|z_j|^4 - q|z_k|^4 - r|z_j|^2|z_k|^2] - s z_k^3 z_j^{*2}, \tag{35}$$

where $j,k=1,2$, $j\neq k$, $A=2a+c$, and $B=2(a+b+c)$. We do not present here an explicit form of the fifth order coefficients p, q, r, and s since it is not important in the further analysis.

Let us first neglect the fifth order terms in Eqs. (35). Then the solutions corresponding to the antiphase periodic oscillations of the modal intensities with the same wave forms but with a phase shift $2\pi/3$ from one mode to the next (periodic AD1 regimes) are given by

$$(z,0),\quad |z|^2=\rho/\mathrm{Re}\, A, \tag{36}$$

$$(0,z),\quad |z|^2=\rho/\mathrm{Re}\, A. \tag{37}$$

The solution (36) is invariant under the transformation $(z_1,z_2)\to e^{-i\vartheta}(e^{i\zeta}z_1,e^{-i\zeta}z_2)$, while the solution (37) is invariant under $(z_1,z_2)\to e^{i\vartheta}(e^{i\zeta}z_1,e^{-i\zeta}z_2)$ with $\vartheta=\zeta=2\pi/3$ and, hence, they have the isotropy subgroup $\tilde{\mathbf{Z}}_3\subset\mathbf{D}_3\times\mathbf{S}^1$ [20].

The eigenvalues determining the stability of the solutions (36) and (37) are

$$\Lambda_{1,2}=-\rho\pm i\sqrt{3(\mathrm{Im}\, A)^2/(\mathrm{Re}\, A)^2-1}, \tag{38}$$

$$\Lambda_{3,4}=\frac{\rho}{\mathrm{Re}\, A}[-\mathrm{Re}\,(2b+c)\pm i\,\mathrm{Im}\, B]. \tag{39}$$

The stability condition $\mathrm{Re}\,\Lambda_{1,2}=-\rho<0$ implies that the AD1 solutions can be stable only if they are supercritical ($\mathrm{Re}\,A>0$). The second pair of eigenvalues (39) describes the stability of the solutions (36) and (37) with respect to small perturbations of the Fourier mode z_2 and z_1, respectively. For $\mathrm{Re}\,A>0$, using the relations (26) and (27), we get the inequality $\mathrm{Re}\,\Lambda_{3,4}<0$ with $\mathrm{Re}\,\Lambda_{3,4}\approx-2\rho\,\mathrm{Re}\,b/\mathrm{Re}\,A=\rho\mathcal{O}(\varepsilon^{-1})$. Hence, in the limit (25), the solutions (36) and (37) are stable if and only if they are supercritical ($\mathrm{Re}\,A>0$). It can also be shown using the asymptotic expressions of the normal form coefficients given in the Appendix that in the limit $\varepsilon\to0$, the condition $\beta>1/4$ is sufficient for the solutions (36) and (37) to be supercritical and stable.

Apart from Eqs. (36) and (37) the third order normal form equations have the following family of periodic solutions:

$$(z,ze^{i\varphi}),\quad |z|^2=\rho/\mathrm{Re}\,(A+B)>0, \tag{40}$$

with constant φ. For $\mathrm{Re}\,(A+B)>0$ Eq. (40) bifurcates supercritically at $\mathcal{H}$. It is stable when $\mathrm{Re}\,(2b+c)<0$. Since in the limit (25) we have $\mathrm{Re}\,(A+B)\approx\mathrm{Re}\,(2b+c)\approx2\mathrm{Re}\,b>0$, the solution (40) is supercritical and unstable.

It can be shown that if the fifth order terms in Eq. (35) are taken into account, the solution (40) splits into two limit cycles with $\varphi=0$ and $\varphi=\pi$. The limit cycle with $\varphi=0$ is invariant under Eq. (34) and, hence, it has the isotropy subgroup $\mathbf{Z}_2(\kappa)\subset\mathbf{D}_3$. For this regime, referred to as AD2 in [10,11], the intensities of two modes have the same wave form and same phase while the third mode is dephased by π. The limit cycle with $\varphi=\pi$ is invariant under the transformation $(z_1,z_2)\to e^{i\pi}(z_2,z_1)$. Therefore, it has the isotropy subgroup $\mathbf{Z}_2(\kappa,\pi)\subset\mathbf{D}_3\times\mathbf{S}^1$ and corresponds to a situation where two modal intensities oscillate with the same wave form but are π out of phase, while the third intensity has a small amplitude oscillation at half the period. It follows from this analysis that for typical values of the parameters for which the experiments are conducted, both limit cycles are unstable near $\mathcal{H}$.

Thus, we have shown that in the limit (25) and for $\mathrm{Re}\,A>0$ only periodic AD1 regimes can be stable near the Hopf bifurcation boundary in a three-mode laser. The stable eigenvalues $\Lambda_{3,4}$ defined by Eq. (39) are associated with antiphased damped oscillations. On the other hand, numerical simulations of Eqs. (1) and (2) indicate that far above $\mathcal{H}$ similar oscillations can become undamped. This corresponds to a secondary Hopf bifurcation which transforms the periodic antiphased AD1 regime into a regime with quasiperiodic modal intensities. An example is presented in Fig. 2. Though such secondary bifurcation far away from the first Hopf bifurcation cannot be described in the framework of the normal form (35), the antiphased properties of the quasiperiodic solutions arising after secondary Hopf bifurcation can be explained using the formalism presented in this paper. One can see that both the carrier and the envelope of the quasiperiodic regime shown in Fig. 2 are of the AD1 type. Since this quasiperiodic regime bifurcates from the AD1 solution with the temporal pattern $\{1,2,3\}$, its carrier is associated with the eigenvector $\mathbf{v}_1$ shown in Fig. 1(a). The envelope of the quasiperiodic solution results from the interaction between the Fourier modes y_1 and y_2. Therefore, depending on the sign of their frequency splitting [$\Delta\omega$ in Eq. (32)], this

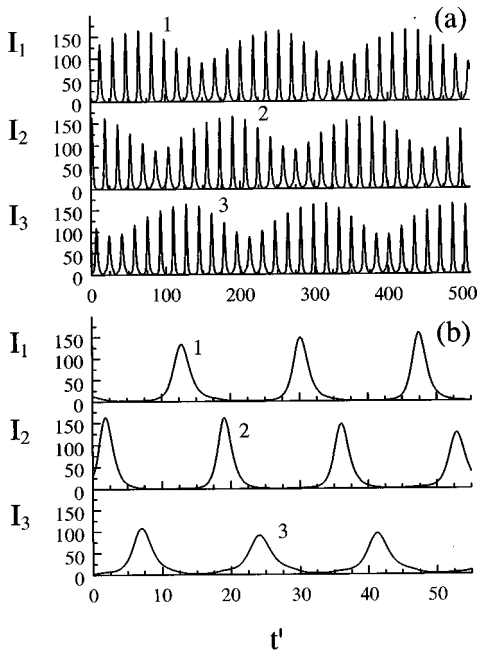

FIG. 2. Quasiperiodic solution of Eqs. (1) and (2) with $N=3$, $\eta=10^{-7}$, $\alpha=10^{-2}$, $\varepsilon=5\times10^{-7}$, $\gamma=43$, $\beta=0.3$, and $t'=t\sqrt{\eta}$. (a) and (b) correspond to the same solution shown on two different time scales. The carrier (envelope) of the quasiperiodic solution is associated with the eigenvector $\mathbf{v}_1$ ($\mathbf{v}_2$) which is shown in Fig. 1(a) and corresponds to the AD1 regime with the temporal pattern $\{1,2,3\}$ ($\{1,3,2\}$).

envelope is associated with either the eigenvector $\mathbf{v}_2$ or the eigenvector $\mathbf{v}_1$. In Fig. 2 the low-frequency antiphased envelope displays the temporal pattern $\{1,3,2\}$ corresponding to the eigenvector $\mathbf{v}_2$. Therefore, in this case we have $\Delta\omega<0$ in Eq. (32). Thus, the appearance of the quasiperiodic regimes can be related to the interaction between different types of periodic antiphased states, each one associated with an eigenvector of the biorthogonal basis of Fourier modes (9). In the subsequent sections we show that for $N\geqslant4$ the normal form equations (23) can exhibit undamped antiphased quasiperiodic oscillations.

VI. FOUR MODES

In the case of four lasing modes, the symmetry group of the normal form equations is generated by

$$\zeta(z_1,z_2,z_3)=(e^{i\zeta}z_1,e^{i2\zeta}z_2,e^{-i\zeta}z_3),\quad \zeta=\frac{\pi}{2},$$

$$\kappa(z_1,z_2,z_3)=(z_3,z_2,z_1),$$

$$\kappa_1\begin{pmatrix}z_1\\z_2\\z_3\end{pmatrix}=\frac{1}{2}\begin{pmatrix}i & 1-i & 1\\1-i & 0 & 1+i\\1 & 1+i & -i\end{pmatrix}\begin{pmatrix}z_1\\z_2\\z_3\end{pmatrix},$$

$$\vartheta(z_1,z_2,z_3)=e^{i\vartheta}(z_1,z_2,z_3),\quad \vartheta\in\mathbf{S}^1.$$

For $N=4$ the third order normal form equations (23) take the form

$$\partial_\tau z_j = z_j[\rho - i\omega - A|z_j|^2 - C|z_2|^2 - B|z_k|^2] - c z_k^2 z_j^* - (c+b) z_2^2 z_k^*, \quad (41)$$

$$\partial_\tau z_2 = z_2[\rho - i\omega - (A+b)|z_2|^2 - C(|z_1|^2 + |z_3|^2)] - 2(c+b) z_1 z_3 z_2^*, \quad (42)$$

where $j,k=1,3$, $j \neq k$, and

$$A = 2a + c, \quad B = 2(a+b+c), \quad C = 2(a+c). \quad (43)$$

Periodic solutions of normal form equations bifurcating from $\mathcal{H}$ can be classified by their invariance properties (isotropy subgroups) [20] . In our analysis we do not distinguish between the solutions belonging to the same group orbit, i.e., which can be obtained from each other with the help of permutations of modal indices. Since all such solutions have identical stability properties it is sufficient to consider only a single representative for each group orbit. It follows from the equivariant Hopf theorem [20] that Eqs. (41) and (42) possess at least five different types of periodic solutions with period $2\pi/\omega$ at $\mathcal{H}$. These solutions are listed below together with their isotropy subgroups:

$$\mathrm{AD1}: (z,0,0), \quad |z|^2 = \rho/\mathrm{Re}\, A, \quad \tilde{\mathbf{Z}}_4, \quad (44)$$

$$\mathrm{AD2}_{31}: (z,z,z), \quad |z|^2 = \rho/\mathrm{Re}\,(6a+3b+7c), \quad \langle \kappa_1 \rangle \times \langle \kappa \rangle, \quad (45)$$

$$\mathrm{AD2}_{22}: (0,z,0), \quad |z|^2 = \rho/\mathrm{Re}\,(A+b), \quad \mathbf{Z}_2 \times \langle \kappa \rangle, \quad (46)$$

$$\mathrm{AD2}_{11}: (z,0,z), \quad |z|^2 = \rho/\mathrm{Re}\,(C+b), \quad \tilde{\mathbf{Z}}_2 \times \langle \kappa \rangle, \quad (47)$$

$$\mathrm{AD1}_3: (z, z - z\sqrt{3}, -2z + \sqrt{3}z), \quad |z|^2 = \rho/[4(2+\sqrt{3})\mathrm{Re}\,(C+a)], \quad \langle (\kappa_1, 2\pi/3) \rangle. \quad (48)$$

Here $\langle \kappa \rangle$, $\langle \kappa_1 \rangle$, $\tilde{\mathbf{Z}}_2$, and $\langle (\kappa_1, 2\pi/3) \rangle$ are the groups generated, respectively, by κ, κ_1, $2\varsigma\vartheta$ with $\vartheta = \pi$, and $\kappa_1 \vartheta$ with $\vartheta = 2\pi/3$. The solution (44) is invariant under cyclic mode permutation and has the isotropy subgroup $\tilde{\mathbf{Z}}_4$. The notation $\mathrm{AD2}_{lm}$ corresponds to the solution with two groups of oscillating modes consisting of l and m modes, respectively. All modal intensities in each group have the identical wave forms and the same phase, while the intensities of the modes belonging to different groups are π out of phase. It follows from the relations (26) and (27) that the solutions (45)–(47) are always supercritical in the limit $\varepsilon \to 0$. The last solution (48) resembles the AD1 solution that appears in a three-mode laser: three of the four modal intensities oscillate with the same wave form and such that each mode is phase shifted by $2\pi/3$ from another mode, while the fourth modal intensity exhibits a small amplitude oscillation with half the period. The stability conditions for all the solutions (44)–(48) can be derived analytically. In the limit (25) the solutions (45)–(48) are unstable with the real parts of the most unstable eigenvalues being $\rho O(\varepsilon^{-1})$.

The eigenvalues determining the stability of the solution (44) are given by Eq. (38) and

$$\Lambda_{3,4} = \frac{\rho}{\mathrm{Re}\, A}[-\mathrm{Re}\, c \pm i\, \mathrm{Im}\, C], \quad (49)$$

$$\Lambda_{5,6} = \frac{\rho}{\mathrm{Re}\, A}[-\mathrm{Re}\,(2b+c) \pm i\sqrt{(\mathrm{Im}\, B)^2 - |c|^2}]. \quad (50)$$

As for $N=3$, the condition $\mathrm{Re}\,\Lambda_{1,2} < 0$ implies that the AD1 solution can be stable only when it is supercritical ($\mathrm{Re}\, A > 0$). Using the asymptotic expressions for the normal form coefficients given in the Appendix, it can be shown that $\mathrm{Re}\, A$ is always positive for $\beta > 1/5$. In the following analysis we assume that the inequality $\mathrm{Re}\, A > 0$ is fulfilled. The eigenvalues $\Lambda_{5,6}$ describe the stability with respect to small perturbations of the Fourier mode z_3. Using the relations (26) and (27) we obtain $\mathrm{Re}\,\Lambda_{5,6} \approx -2\rho\, \mathrm{Re}\, b/\mathrm{Re}\, A < 0$. Finally, the eigenvalues $\Lambda_{3,4}$ describe the stability with respect to small perturbations of the Fourier mode z_2. Since for physical parameter values we have $\mathrm{Re}\, c < 0$ (see the Appendix), these eigenvalues have positive real parts. This means that the AD1 solutions are *unstable* at least near $\mathcal{H}$ where the third order normal form equations are valid. This is in agreement with the results of numerical simulations of the normal form equations (41) and (42). For parameter values relevant to experimental situations, these equations exhibit quasiperiodic oscillations with two frequencies, one of them being determined by the Hopf frequency ω and the second being equal to the frequency splitting of the Fourier modes z_1 and z_2. In the limit (25) using the inequality $|\mathrm{Re}\, a|, |\mathrm{Re}\, c| \ll |\mathrm{Re}\, b|, |\mathrm{Im}\, a|, |\mathrm{Im}\, b|, |\mathrm{Im}\, c|$ which is the consequence of Eq. (26), the quasiperiodic solution of Eqs. (41) and (42) can be approximated as

$$|z_1|^2 \approx \frac{\rho}{\mathrm{Re}\, A} + O(\varepsilon), \quad |z_2|^2 \approx 2|z_1|^2 D_- F + O(\varepsilon^2), \quad |z_3|^2 \approx |z_1|^2 D_+ D_- F^2 + O(\varepsilon^3), \quad (51)$$

$$\arg z_1 - \arg z_2 = \Delta\omega\, \tau \approx \tau[|z_1|^2\, \mathrm{Im}\, c + O(\varepsilon^{1/2})], \quad (52)$$

$$\sin(\arg z_1 + \arg z_3 - 2\arg z_2) \approx \left(\frac{3\, \mathrm{Im}\, c\, \mathrm{Re}\, b}{2\sqrt{D_+ D_-}} \right) |z_1|^2\, \mathrm{Im}\, c + O(\varepsilon^{3/2}), \quad (53)$$

where

$$F = -\frac{2\, \mathrm{Re}\, c}{(3\mathrm{Im}\, c)^2 \mathrm{Re}\, b},$$

$$D_\pm = (\mathrm{Re}\, b)^2 + [\mathrm{Im}\,(4b + c \pm 3c)/4]^2. \quad (54)$$

It is seen from the data shown in Fig. 3 that in the limit (25) these expressions are in good agreement with the results of numerical integration of Eqs. (41) and (42). Using Eqs. (51)–(54) and the relations (26), we get the asymptotic expressions $|z_2|^2 = |z_1|^2 O(\varepsilon)$ and $|z_3|^2 = |z_1|^2 O(\varepsilon^2)$ for the quasiperiodic solution. Therefore, this solution is characterized by the hierarchy $|z_1| \gg |z_2| \gg |z_3|$, which can be interpreted in the following way. Let us consider the secondary Hopf bifurcation of the AD1 solution (44) leading to a qua-

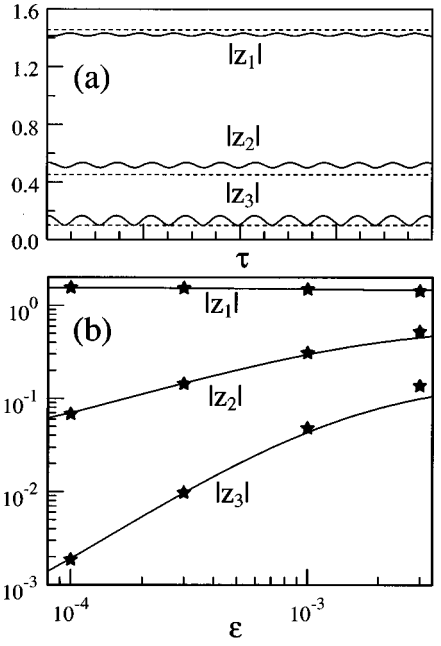

FIG. 3. Quasiperiodic solutions of the normal form equations. $N=4$, $\rho=0.2$. The normal form coefficients are evaluated at $\eta=0.001\,25$, $\alpha=0.03$, and $\beta=0.3$. (a) $\varepsilon=0.003$. The solid lines correspond to numerical solution of Eqs. (41) and (42). The dashed lines are obtained using the approximate expressions (51)–(53). (b) The solid lines correspond to the approximate solution (51)–(53) which are constant in time. The asterisks denote the time-averaged numerical solutions of Eqs. (41) and (42).

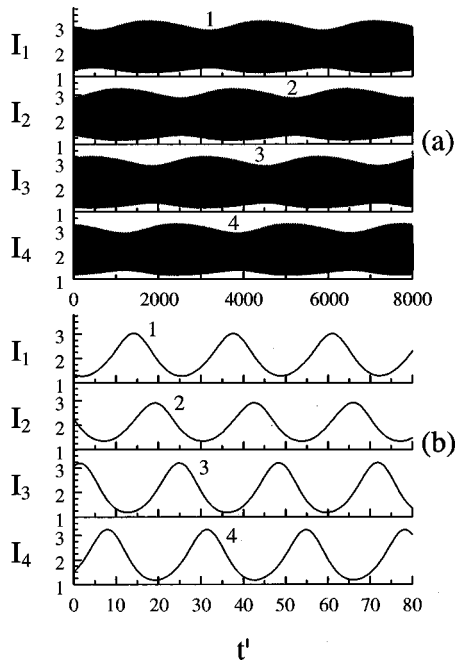

FIG. 4. Quasiperiodic solution of Eqs. (1) and (2) with $N=4$ and $\gamma=0.355$. The values of the parameters η, α, ε, and β are the same as in Fig. 3(a), and $t'=t\sqrt{\eta}$. (a) and (b) correspond to the same solution shown on two different time scales. The carrier (envelope) of the quasiperiodic solution is associated with the eigenvector $\mathbf{v}_1$ ($\mathbf{v}_3$) which is shown in Fig. 1(b) and corresponds to the AD1 regime of the type {1,2,3,4} ({1,4,3,2}).

siperiodic solution that takes place at $\mathrm{Re}\,\Lambda_{3,4}=0$ ($\mathrm{Re}\,c=0$). At this boundary the antiphase oscillations associated with the Fourier mode z_2 become undamped, leading to a weak antiphased modulation of the solution (44). The modulation frequency is determined by the frequency splitting of the Fourier modes z_2 and z_1. This frequency vanishes at $\mathcal{H}$. Since for $\mathrm{Re}\,c=0$ we have $F=0$ in Eq. (54) and hence $z_2=z_3=0$ in Eq. (51), it becomes clear that the relations (51)–(54) describe the quasiperiodic solution bifurcating from the AD1 solution at the secondary bifurcation boundary $\mathrm{Re}\,\Lambda_{3,4}=0$. Moreover, the relations (26) imply the asymptotic expressions $\mathrm{Re}\,\Lambda_{3,4}=\rho O(1)$, $\mathrm{Re}\,\Lambda_{5,6}=\rho O(\varepsilon^{-1})$, and, hence, the relation $\mathrm{Re}\,\Lambda_{3,4}/\mathrm{Re}\,\Lambda_{5,6}=O(\varepsilon)$. Therefore, the hierarchial property of the quasiperiodic solution can be related to the fact that the effective distance from the secondary Hopf bifurcation threshold $\mathrm{Re}\,\Lambda_{3,4}=0$ becomes very small in the limit $\varepsilon\to 0$ (the secondary bifurcation itself is not accessible in physical situations since $\mathrm{Re}\,c$ is always negative). This is why in the limit (25) the contributions of the Fourier modes z_2 and z_3 in Eqs. (51)–(54) vanish and the quasiperiodic solution (51)–(54) becomes very similar to the periodic AD1 solution (44). Since $F>0$ according to Eq. (27), and $D_{\pm}>0$, we can conclude from Eq. (51) that the quasiperiodic solution (51)–(54) bifurcates supercritically at the secondary Hopf bifurcation threshold $\mathrm{Re}\,\Lambda_{3,4}=0$ and, therefore, is stable near this threshold.

Let us examine the temporal pattern associated with the antiphased envelope of the quasiperiodic solution (51)–(54). Since this solution bifurcates from the AD1 solution (44), its carrier is determined by the eigenvector $\mathbf{v}_1$ which is associated with the dominating Fourier mode z_1 and the temporal pattern {1,2,3,4}. According to the results of Sec. IV B, the envelope of the quasiperiodic solution resulting from the interaction of the Fourier modes z_1 and z_2 is associated either with the eigenvector $\mathbf{v}_3$ [$\Delta\omega<0$ in Eq. (32)] or with the eigenvector $\mathbf{v}_1$ [$(\Delta\omega>0$ in Eq. (32)]. Since according to Eqs. (52) and (27) $\Delta\omega\approx|z_1|^2\,\mathrm{Im}\,c<0$, the frequency splitting of the Fourier modes z_1 and z_2 is negative, and the envelope of the quasiperiodic solution (51)–(53) corresponds to the eigenvector $\mathbf{v}_3$ and the temporal pattern {1,4,3,2}. This is in agreement with the results of a numerical integration of the original laser equations. Figure 4 presents a quasiperiodic

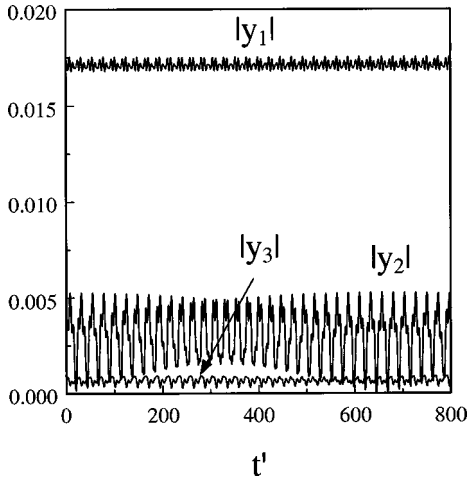

FIG. 5. Same solution as in Fig. 4 presented using the coordinates $y_{1,2,3}$ defined by Eq. (13).

solution of Eqs. (1) and (2) calculated near $\mathcal{H}$ for the parameter values of Fig. 3. The initial conditions were chosen in such a way that the carrier of this solution has the temporal pattern {1,2,3,4}. The envelope of the quasiperiodic solution shown in Fig. 4 has the temporal pattern {1,4,3,2} as predicted by the normal form analysis. In Fig. 5 the same solution is represented using the Fourier modes $y_{1,2,3}$ which in the linear approximation coincide with $z_{1,2,3}$. As for the solution of the normal form equations shown in Fig. 3(a), the Fourier mode y_1 determining the carrier type of the quasiperiodic solution dominates the hierarchy. The second dominating mode is y_2, which determines the envelope type of the quasiperiodic solution ($\mathbf{v}_3$). The smallest Fourier mode y_3 turns out to be of the same order as y_4, which is not shown in Fig. 5. The amplitude y_4 determines the oscillation depth of the total output laser intensity.

Thus, we see that in a laser operating in four identical modes, pure periodic AD1 regimes are always *unstable* in the vicinity of $\mathcal{H}$ if $\beta > 1/5$ and in the limit (25). Instead of these regimes the third order normal form equations predict quasiperiodic hierarchical solutions characterized by antiphased carrier and antiphased envelope. However, according to our numerical observations the width of the applicability domain of the third normal form equations (23) decreases with the decrease of the parameters ε and η. There exist at least two reasons for this phenomenon. The first one is that due to the singular nature of the laser equations (1) and (2) in the limit (25), $\mathcal{H}$ is a singular Hopf bifurcation [28]. Very recently the singular nature of a Hopf bifurcation was also established in a model of a solid-state laser operating on n-Λ transition. It was shown that the asymptotic expansions used in the Hopf bifurcation analysis are valid only for $\rho \ll \eta^{1/2}$ [29]. This conclusion is supported by the results of numerical simulations of Eqs. (1) and (2), which show that the quasiperiodic solution arising at the primary instability threshold $\mathcal{H}$ can disappear via a secondary Hopf bifurcation of the corresponding AD1 solution. After such a bifurcation, which cannot be described by the third order normal form equations (23), the AD1 solution becomes stable. Moreover, we have found that as the parameter ε becomes smaller, the distance between $\mathcal{H}$ and the secondary Hopf bifurcation decreases. However, according to our numerical results, the stable AD1 regime arising after this secondary Hopf bifurcation usually undergoes a tertiary Hopf bifurcation leading once again to a quasiperiodic solution with antiphased properties similar to those predicted using our normal form analysis. This indicates that the qualitative conclusions derived with the help of the normal form method can remain valid even beyond the applicability domain of the normal form equations (23). Moreover, far above the first instability threshold $\mathcal{H}$, we have observed numerically 3D tori with the carrier corresponding to the eigenvector $\mathbf{v}_1$ and two antiphased envelopes corresponding to the eigenvectors $\mathbf{v}_3$ and $\mathbf{v}_2$. This result indicates that when the linear gain parameter is large enough, the antiphased oscillations associated with the complex eigenvalues $\Lambda_{5,6}$ describing the stability with respect to small perturbations of the Fourier mode z_3 can become unstable. These oscillations produce an additional antiphased low-frequency envelope which exhibits a temporal pattern associated with the eigenvector $\mathbf{v}_2$ displayed in Fig. 1(b).

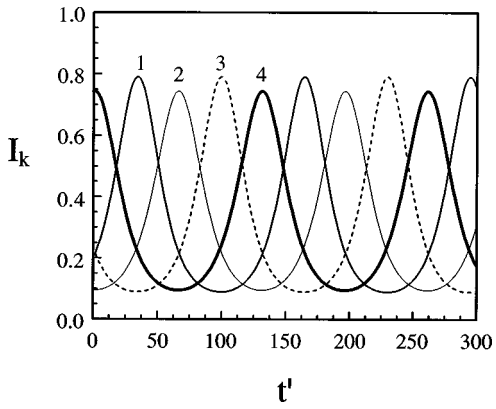

FIG. 6. Stable periodic solution of Eqs. (1) and (2) with broken $\tilde{\mathbf{Z}}_N$ symmetry. $N=4$, $\eta=10^{-6}$, $\alpha=0.01$, $\varepsilon=0.96\times10^{-5}$, $\gamma=0.0151$, $\beta=0.2$, and $t'=t\sqrt{\eta}$.

The second factor that restricts the applicability of the normal form equations is related to the possibility of synchronization of the quasiperiodic solution. According to Eqs. (7) and (8) in the limit (25) the Hopf bifurcation frequency becomes $\omega = O(\varepsilon^{-1/2})$. On the other hand, taking into account the asymptotic expressions for the normal form coefficients given in the Appendix, we conclude that the envelope frequency of the quasiperiodic solution (51)–(53) is $|\Delta\omega| \approx |z_1|^2 \operatorname{Im} c = \rho O(\varepsilon^{-3/2})$. Hence, for $\varepsilon \to 0$ the envelope frequency grows much faster than the carrier frequency ω. However, since the normal form equations (20) and (23) are valid only for $|\Delta\omega| \ll \omega$, for ε small enough the applicability domain of the normal form equations becomes very narrow, $\rho \ll \varepsilon = O(\eta)$. Outside this domain the carrier and the envelope frequencies can be of the same order and, hence, the synchronization phenomenon which cannot be described by the normal form equations (20) and (23) is possible.

For $N=4$ we have a simple pair of pure imaginary eigenvalues at the secondary Hopf bifurcation boundary $\operatorname{Re}\Lambda_{3,4} = 0$. Therefore, each of the AD1 solutions generates only a single 2D torus. Therefore, one could expect that generically the total number of different stable hierarchical quasiperiodic solutions obtained by permutations of the modal indices coincides with the total number of different periodic AD1 regimes, i.e., $(4-1)!=6$. However, simple considerations indicate that synchronization of these tori may produce a greater number of stable periodic solutions. Indeed, a synchronization of the quasiperiodic solution characterized by the hierarchy $|z_1| \gg |z_2| \gg |z_3|$ would produce periodic solutions with all three nonzero amplitudes. Neglecting the contribution of the smallest Fourier mode z_3, we conclude that the periodic antiphased regime arising after synchronization corresponds to the linear combination $z_1\mathbf{v}_1 + z_2\mathbf{v}_2$, where the phase difference between the Fourier modes z_1 and z_2 is fixed for a pure periodic solution. Though for $|z_1| \gg |z_2|$ such solutions are very similar to the AD1 solutions which are invariant under the isotropy subgroup $\tilde{\mathbf{Z}}_4$, the presence of the second Fourier mode $z_2 \neq 0$ breaks the symmetry with respect to cyclic permutations of modal indices. Therefore, in this case such permutations also can produce distinct periodic solutions. In particular, the symmetry breaking associated with the synchronization of the hierarchical quasiperiodic solution can lead to slightly different oscillation amplitudes for dif-

ferent modes. Similar periodic solutions were observed numerically and one of them is presented in Fig. 6. In this figure two pairs of modes have slightly different oscillating amplitudes. The existence of such a solution will imply from symmetry considerations the existence of at least $2(4-1)!=12$ distinct stable solutions which can be obtained with the help of modal index permutations. Stable periodic solutions for which all four modes have slightly different oscillation amplitudes were also observed for parameters close to those of Fig. 6. In this case, the number of stable solutions obtained by permutations of the modal indices increases up to $4!=24$.

VII. FIVE OR MORE MODES

In this section we restrict our considerations to the stability properties of the antiphased AD1 solutions of Eqs. (23) having the isotropy subgroup $\tilde{\mathbf{Z}}_N$. All such solutions belong to the same group orbit and, hence, without loss of generality we can consider only a single solution defined by

$$|z_1|^2=\rho/\mathrm{Re}\,A, \quad z_k=0 \quad (k>1). \tag{55}$$

The first two pairs of eigenvalues determining the stability of the solution (55) are given by Eqs. (38) and (49). As in the case $N=4$, the eigenvalues $\Lambda_{1,2}$ determine whether the AD1 regime bifurcates supercritically or not. It can be shown that in the limit (25) the condition $\beta<1/(N+1)$ is sufficient for the AD1 solution to be supercritical. This corresponds to $\mathrm{Re}\,A>0$ and we will assume that this inequality is fulfilled. Since we have $\mathrm{Re}\,c<0$, the second pair of eigenvalues $\Lambda_{3,4}$, which describes the stability with respect to small perturbations of the Fourier mode z_2, is always unstable. For $N=5$ the remaining four eigenvalues are given by

$$\Lambda_{5,7}=\frac{\rho}{\mathrm{Re}\,A}[-b-\mathrm{Re}\,c\pm i\sqrt{(\mathrm{Im}\,C-ib)^2-|c|^2}], \tag{56}$$

$$\Lambda_{6,8}=\Lambda_{5,7}^{*}. \tag{57}$$

For $N\geqslant 6$ there exist $N-5$ additional pairs of complex eigenvalues

$$\Lambda_{9,10}=\frac{\rho}{\mathrm{Re}\,A}[-\mathrm{Re}\,c\pm i\sqrt{(\mathrm{Im}\,C)^2-|c|^2}]. \tag{58}$$

Here A, B, and C are defined by Eq. (43). The eigenvalues (56) and (57) describe the stability with respect to small perturbations of the Fourier modes z_3 and z_{N-1}. In the limit (25) the eigenvalues $\Lambda_{5,6}$ have negative real parts.

We have found that for $N=5$, depending on the sign of the real parts of the eigenvalues $\Lambda_{7,8}$, the normal form equations can exhibit two different types of behavior. If $\mathrm{Re}\,\Lambda_{7,8}<0$, the only unstable eigenvalues are $\Lambda_{3,4}$. In this case the solutions of the normal form equations (23) are quasiperiodic and characterized by a hierarchy similar to that obtained for $N=4$. Specifically, for the hierarchical solution with dominating Fourier mode z_1, the second dominating mode which determines the type of low-frequency modulation of modal intensities is z_2. Hence, depending on the sign of the frequency splitting of the Fourier modes z_1 and z_2, this envelope is associated either with the eigenvector $\mathbf{v}_4$ or with $\mathbf{v}_1$.

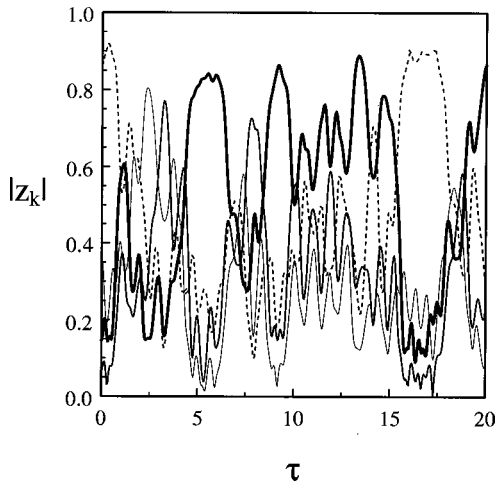

FIG. 7. Numerical solution of the normal form equations (23) with $N=5$, $\rho=0.2$. The normal form coefficients are evaluated at $\eta=10^{-4}$, $\alpha=0.02$, $\varepsilon=5\times10^{-4}$, and $\beta=0.34$.

However, $\mathrm{Re}\,\Lambda_{7,8}>0$ in most physical situations. In this case quasiperiodic hierarchical solutions are unstable and numerical integration of Eqs. (23) yields more complicated irregular solutions as shown in Fig. 7. This kind of solution can be related to a chaotic intermittency between different unstable quasiperiodic states, each associated with a certain AD1 regime. Similar antiphased solutions with slowly varying irregular envelope were observed by numerical integration of Eqs. (1) and (2) close to $\mathcal{H}$. They are presented in Figs. 8 and 9. Unlike the hierarchical quasiperiodic solution described above, for which the carrier type does not change with time, the solution shown in Fig. 9 has a high-frequency carrier with a *time-dependent* temporal pattern. This intermittent behavior is similar to the chaotic itineracy found in [21].

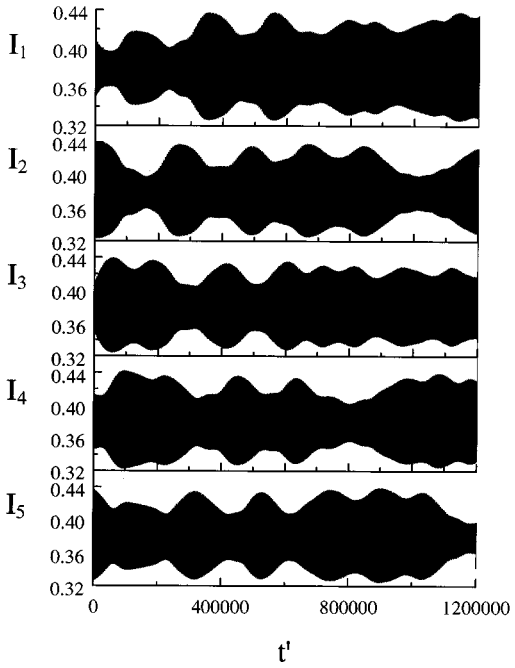

FIG. 8. Antiphased solution of Eqs. (1) and (2) with slowly varying irregular envelope. $N=5$, $\gamma=0.04111$, and $t'=t\sqrt{\eta}$. Other parameter values are the same as for Fig. 7.

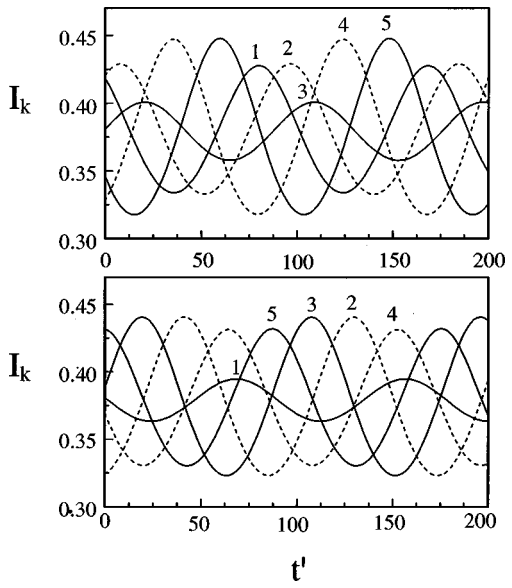

FIG. 9. Same solution as in Fig. 8 shown on two identical time intervals separated by $\Delta t' = 89\,800$. The local maxima of the intensity I_k are labeled k.

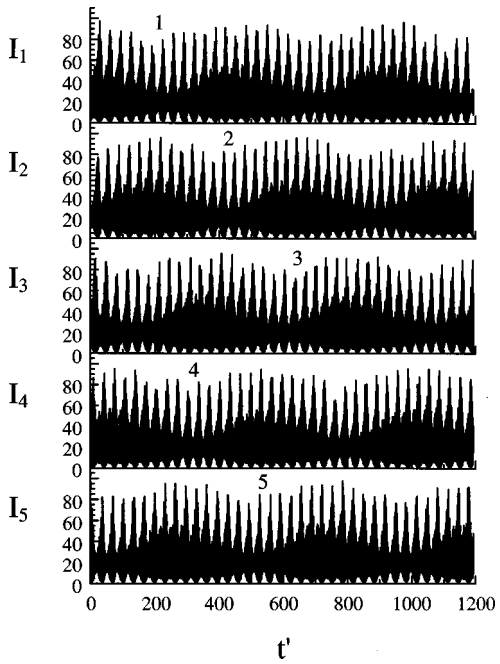

FIG. 10. Quasiperiodic solution of Eqs. (1) and (2) with $N=5$, $\eta=10^{-7}$, $\alpha=10^{-2}$, $\varepsilon=3\times10^{-7}$, $\gamma=0.43$, $\beta=0.3$, and $t'=t\sqrt{\eta}$. The envelope corresponding to the smallest of the three frequencies is associated with the eigenvector $\mathbf{v}_2$ shown in Fig. 1(c). This eigenvector corresponds to the antiphased AD1 regime of the type $\{1,4,2,5,3\}$.

As in the case $N=4$, stable AD1 solutions can appear for $N=5$ by increasing the distance from $\mathcal{H}$. Usually they appear in the following way. First, the quasiperiodic hierarchical solutions become stable. After that, these solutions merge into the AD1 solutions at the secondary Hopf bifurcation point. However, when the distance from $\mathcal{H}$ is further increased, the AD1 solutions usually become unstable again via a tertiary Hopf bifurcation leading to quasiperiodic solutions with the antiphased properties that can still be described qualitatively using the orthogonal Fourier basis (9). If, for example, the antiphased carrier type of the quasiperiodic regime corresponds to the eigenvector $\mathbf{v}_1$, the envelope type is determined by one of the remaining eigenvectors. Our numerical simulations also indicate the existence of solutions with two antiphased envelopes appearing on different time scales. Such solutions, obtained by numerical integration of Eqs. (1) and (2) with $N=5$, are displayed in Figs. 10 and 11. One can see from these figures that while the antiphased carrier of the solution corresponds to the eigenvector $\mathbf{v}_1$ and the temporal pattern $\{1,2,3,4,5\}$, the two antiphased envelopes correspond to the eigenvectors $\mathbf{v}_4$ with mode pattern $\{1,2,3,4,5\}$ and $\mathbf{v}_2$ with mode pattern $\{1,5,4,3,2\}$. It follows from our analysis that these envelopes can be related to the eigenvalues $\Lambda_{3,4}$ and $\Lambda_{5,6,7,8}$, respectively.

Finally, for $N\geqslant 6$ there are $N-5$ pairs of the eigenvalues (58), each of them describing the stability with respect to small perturbations of the Fourier modes z_{3+k} and z_{N-2-k} with $k\leqslant N-5$. Since $\mathrm{Re}\, c<0$, these eigenvalues have positive real parts. Therefore, at least in the vicinity of $\mathcal{H}$ the number of unstable eigenvalues of the AD1 solution increases with the mode number N. This may be one of the main obstacles that prevents the observation of the pure periodic AD1 regimes in a frequency-doubled laser with large number of modes.

The stability analysis of the solution (55) performed using the normal form equations (23) is valid only in the vicinity of $\mathcal{H}$. However, Eqs. (14) governing the evolution of the variables y_j are isomorphic to Eqs. (1) and (2) if $\omega^2>0$ in Eq. (8). As already mentioned, the variable y_j can be considered as a Fourier mode corresponding to the wave number $K_j = j - N/2$. Now let us return to the expression (32) describing the envelope of a quasiperiodic solution which arises after a secondary Hopf instability of the AD1 solution (55). It follows from this expression that the temporal pattern of the envelope is determined by the wave number difference of the Fourier modes y_1 and y_{m+1} and by the sign of their frequency splitting $\Delta\omega$. Hence, there exists a correspondence between the envelope pattern of the quasiperiodic solution and the wave number splitting of the basic Fourier mode y_1 and the second dominating (most unstable) Fourier mode y_{m+1}. We illustrate this statement by Fig. 12 which shows the same quasiperiodic solution as in Figs. 10 and 11, but presented using the antiphased Fourier basis $y_1, \ldots, y_5$. It is seen that the basic Fourier mode determining the carrier type of the quasiperiodic solution is the mode y_1. The second (third) dominating Fourier mode y_2 (y_3) produces the envelope associated with the eigenvector $\mathbf{v}_4$ ($\mathbf{v}_2$). According to Figs. 10 and 11, both the Fourier modes y_2 and y_3 produce undamped oscillations and, therefore, they are unstable. It can be seen from Fig. 12 that the most unstable secondary Fourier mode is the mode y_2. It is associated with the wave number closest to that of the basic Fourier mode y_1 ($K_2 - K_1 = 1$). This indicates that the first instability of the AD1 solution is associated with the *longest wavelength* perturbations. It should be noted that we have observed a similar feature in almost all cases where the secondary Hopf bifurcations of the AD1 solutions have been detected by numerical integration of Eqs. (1) and (2). In Fig. 12 the Fourier mode y_4 with $K_4 = -K_1$ has the smallest absolute value. This could be interpreted as a result of strong competition

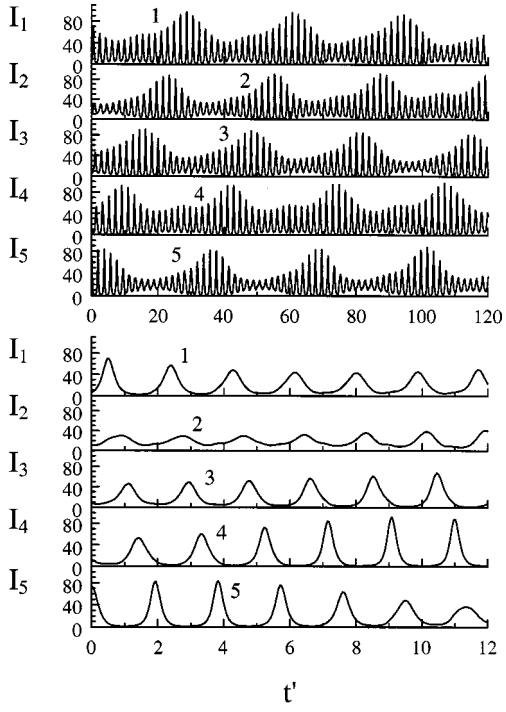

FIG. 11. Same as Fig. 6 but on a larger time scale. The envelope corresponding to the second smallest frequency is associated with the temporal pattern {1,5,4,3,2}. The oscillations with the carrier frequency are associated with the temporal pattern {1,2,3,4,5}.

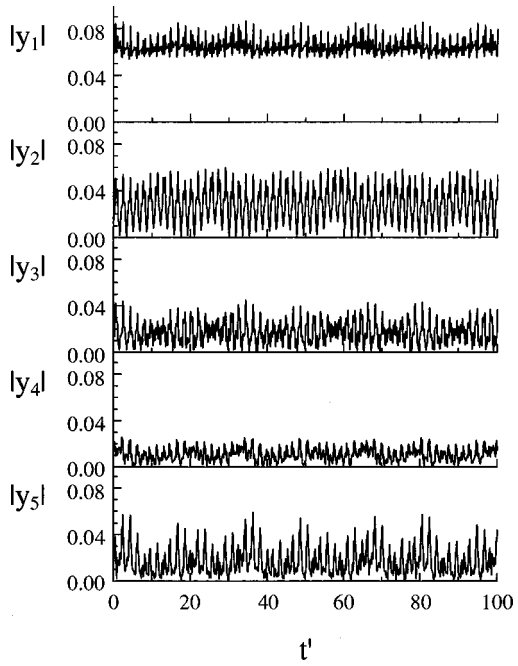

FIG. 12. Same solution as in Figs. 10 and 11, but presented in the antiphased Fourier basis.

between the counterpropagating waves with equal absolute values of group velocities.

VIII. CONCLUSION

We have studied the $(N-1)$-fold degenerate Hopf bifurcation that is responsible for the onset of the antiphase oscillations in a model of intracavity second harmonic generation. Using the normal form techniques and symmetry considerations, we have derived third order normal form equations (23) and (28) describing the mode interaction near the instability threshold. Since the normal form equations obtained are universal, they can be applied to study not only the ISHG problem but also an equivariant Hopf bifurcation in other systems consisting of globally coupled identical elements. With the help of these equations we have performed an analytical stability analysis of periodic solutions emerging at $\mathcal{H}$. Specifically, in the parameter range typical of experiments, we have shown that if the mode number N is greater than 3, the usual periodic AD1 solutions characterized by equal phase shift $2\pi/N$ between neighboring modes are usually *unstable* in the vicinity of $\mathcal{H}$. Moreover, the number of unstable eigenvalues for these solutions increases with the increase of the mode number N. This might prevent the observation of the pure periodic AD1 regimes in a frequency-doubled laser with large number of excited modes. Note that for $N>3$ the instability of the AD1 solution is accompanied by the appearance of a *strong resonance* in the normal form equations [20,24].

The comparison of the analytical results with those of numerical simulations of the original laser equations shows that though in the limit (25) the validity domain of the third order normal form equations (23) is very narrow, antiphased quasiperiodic oscillations similar to those predicted using the normal form method can be observed even far above the Hopf instability threshold. These solutions are characterized by antiphased carrier and low-frequency antiphased envelopes, each of them corresponding to an eigenvector of the biorthogonal basis (9)–(11). Such kinds of regimes can be interpreted as a result of interaction between different antiphased states (Fourier modes) oscillating with slightly different frequencies and corresponding to different wave numbers. According to this interpretation the frequency and the temporal pattern of the antiphased envelope are determined by the wave number difference and the frequency splitting of the corresponding interacting Fourier modes each associated with a certain antiphase state.

It follows from our analysis that the coefficients of the normal form equations governing the evolution of modal intensities near $\mathcal{H}$ obey the asymptotic scalings (26). This implies the existence of a certain hierarchy between the real parts of the eigenvalues determining the stability of the AD1 regime, with some eigenvalues having absolute values of their real parts much smaller than the others. Therefore, one could expect that the relaxation frequencies associated with the eigenvalues having the smallest absolute values of their real parts might be detected in the fluctuation spectra of a stable AD1 regime which can appear at a finite distance from $\mathcal{H}$. For $\mathrm{Re}\,c=0$ in Eqs. (23) and (28), the AD1 solution of the normal form equations is neutrally stable with the number of neutrally stable eigenvalues increasing linearly with N. A related property, referred to as neutral stability of the splay-phase solution, has been reported in Josephson junction arrays [30,31] and in an array of linearly coupled solid-state lasers [16]. In our model, instead of neutrally stable directions we have weakly unstable directions which correspond to eigenvalues having real parts of the order $\rho O(\varepsilon^0)$. Numerical simulations of Eqs. (1) and (2) show that the

weakly unstable directions can be stabilized by increasing the distance from $\mathcal{H}$ and, as a result of this, stable AD1 solutions can appear. In the parameter range (25) we have not observed this stabilization for the mode numbers $N>5$.

We have also presented numerical evidence for a stable solution with slightly broken symmetry under cyclic permutations of modal indices which could be related to the synchronization on the antiphased torus. It follows from symmetry considerations that the number of such stable solutions should be greater than the number of the usual AD1 periodic regimes, which is equal to $(N-1)!$.

ACKNOWLEDGMENTS

This research has been supported in part by the Fonds National de la Recherche Scientifique, the Interuniversity Attraction Pole program of the Belgian government, and by an INTAS grant.

APPENDIX: COEFFICIENTS OF THE NORMAL FORM

The coefficients in Eqs. (23) evaluated up to a common positive multiplicator are

$$\mathrm{Re}\,a=\frac{(1-\beta)\,\theta\{\theta N\beta\,\omega^2+[1-\theta(1-\beta)]\,(N^2-\omega^2+\Omega^2)\}}{2(N^2+\Omega^2)},$$

$$\mathrm{Im}\,a=\frac{\theta(1-\beta)\,\{\theta N(2-3\,\beta)\,\omega^2+[2\,\theta(1-\beta)-\omega^2]\,(N^2-\omega^2+\Omega^2)\}}{2\,\omega(N^2+\Omega^2)},$$

$$\begin{aligned}\mathrm{Re}\,b=&\frac{1}{2\,[N^2+(2\,\omega-\Omega)^2]\,[N^2+(2\,\omega+\Omega)^2]}(N\,\omega^2\,\{8\,\theta^2(1-\beta^2-\theta N\,(1-\beta)\,[11-\theta\,(3+\beta)]-4\,\omega^2[1+5\,\theta-6\,\theta\,\beta\\&-\theta^2\,(1-\beta)^2]+N\omega^2\,[11+5\,\theta-17\,\theta\,\beta+4\,\theta^2\beta(1-\beta)]+8\,\omega^4\,(1-\theta\beta)+\theta\,(N^2+\Omega^2)\,[2-3\beta+2\beta\omega^2-2\,\theta(1-\beta)^2]\}\\&+[1-\theta(1-\beta)][\omega^2-\theta(1-\beta)]\,(N^4+4\omega^4+2\,N^2\Omega^2-5\,\omega^2\,\Omega^2+\Omega^4)),\end{aligned}$$

$$\begin{aligned}\mathrm{Im}\,b=&\frac{1}{6\,\omega\,[N^2+(\Omega-2\,\omega)^2]\,[N^2+(\Omega+2\,\omega)^2]}(-12\,N\,\omega^4\,\{\theta\,(1-\beta)(3-\theta)-\omega^2[3+\theta-4\,\theta\beta+\theta^2\beta(1-\beta)]\}\\&+3\,\theta N\,\omega^2\,\{(7\,\beta-4)\,\omega^2+\theta\,(1-\beta)\,[2-\beta\,(3+\omega^2)]\}\,(N^2+\Omega^2)+[\omega^2+3\,\theta\,(1-\beta)\,\omega^2-2\,\omega^4\\&+\theta^2(1-\beta)^2\,(\omega^2-2)]\,(N^4+4\,\omega^4-5\,\omega^2\,\Omega^2+\Omega^4)-N^2\omega^2\,(2\,\omega^2-1)\,(11\,\omega^2+2\,\Omega^2)\\&+3\,\theta\,N^2\omega^2\,[(19-23\,\beta)\,\omega^2+8\,\beta\,\omega^4+2\,(1-\beta)\,\Omega^2]-\theta^2N^2\,(1-\beta)^2\,[13\,\omega^4+4\,\Omega^2+2\,\omega^2\,(11-\Omega^2)]),\end{aligned}$$

$$\mathrm{Re}\,c=-\frac{1}{2}(1-\beta)\,\theta[1-\theta(1-\beta)]<0,$$

$$\mathrm{Im}\,c=\frac{-\omega^2(1+\omega^2)+\theta(1-\beta)\,[3\,\omega^2-\theta(1-\beta)\,(10+\omega^2)]}{6\,\omega}.$$

Here ω and Ω are defined by Eqs. (8).

In the limit (25), we have obtained the following asymptotic expressions:

$$\mathrm{Re}\,a=\frac{N\theta\,\beta(1-\beta)}{2[1+(N-1)\beta]}+O(\varepsilon),$$

$$\mathrm{Im}\,a=-\frac{N\theta\beta(1-\beta)}{2[1+(N-1)\,\beta]}\left(\frac{\alpha\,(1-\beta)\,\theta}{\varepsilon I_0}\right)^{1/2}+O(\varepsilon^{1/2}),$$

$$\mathrm{Re}\,b=\frac{N\,\alpha\,(1-\beta)\,\theta\{8(1-\beta)^2-\beta[3-(N+3)\,\beta]\,[1+\theta(1-\beta)]\}}{2\varepsilon I_0[3-(N+3)\beta]^{\,2}}+O(1),$$

$$\mathrm{Im}\,b=\frac{N\beta}{3[3-(N+3)\,\beta]}\left(\frac{\alpha\,(1-\beta)\,\theta}{\varepsilon I_0}\right)^{3/2}+O(\varepsilon^{-1/2}),$$

$$\mathrm{Im}\, c = -\frac{1}{6}\left(\frac{\alpha(1-\beta)\theta}{\varepsilon I_0}\right)^{3/2} + O(\varepsilon^{-1/2}),$$

where I_0 is defined in Eq. (4).

[1] P. Hadley and M.R. Beasley, Appl. Phys. Lett. **50**, 621 (1987).
[2] K. Wiesenfeld and P. Hadley, Phys. Rev. Lett. **62**, 1335 (1989).
[3] K. Yoshimoto, K. Yoshikawa, Y. Mori, and I. Hanazaki, Chem. Phys. Lett. **189**, 18 (1992).
[4] W.J. Freeman and C.A. Skarda, Brain Res. Rev. **10**, 47 (1985).
[5] K. Wiesenfeld, C. Bracikowski, G. James, and R. Roy, Phys. Rev. Lett. **65**, 1749 (1990).
[6] C. Bracikowski and R. Roy, Chaos **1**, 49 (1991).
[7] K. Otsuka, Phys. Rev. Lett. **67**, 1090 (1991).
[8] S. Bielawski, D. Derozier, and P. Glorieux, Phys. Rev. A **46**, 1692 (1992).
[9] J.-Y. Wang and P. Mandel, Phys. Rev. A **48**, 671 (1993).
[10] J.-Y. Wang, P. Mandel, and T. Erneux, Quantum Semiclassic. Opt. **7**, 169 (1994).
[11] J.-Y. Wang and P. Mandel, Phys. Rev. A **52**, 1474 (1995).
[12] P. Mandel, *Theoretical Problems in Cavity Nonlinear Optics* (Cambridge University Press, Cambridge, England, 1997).
[13] V.I. Ustyugov, O.A. Orlov, M.M. Khaleev, G.E. Novikov, E.A. Viktorov, and P. Mandel, Appl. Phys. Lett. **71**, 154 (1997).
[14] S. Falter, K.-M. Du, Y. Liao, M. Quade, J. Zhang, P. Loosen, and R. Poprawe, Opt. Lett. **22**, 609 (1997).
[15] G. Huyet, S. Balle, M. Giudici, C. Green, G. Giacomelli, and J.R. Tredicce, Opt. Commun. **149**, 341 (1998).
[16] M. Silber, L. Fabiny, and K. Wiesenfeld, J. Opt. Soc. Am. B **10**, 1121 (1993).
[17] K.Y. Tsang, R.E. Mirollo, S.H. Strogatz, and K. Wiesenfeld, Physica D **48**, 102 (1991).
[18] D.G. Aronson, M. Golubitsky, and J. Mallet-Paret, Nonlinearity **4**, 903 (1991).
[19] R.-D. Li and T. Erneux, Phys. Rev. A **49**, 1301 (1994).
[20] M. Golubitsky, I. Stewart, and D.G. Schaeffer, *Singularities and Groups in the Bifurcation Theory* (Springer-Verlag, New York, 1988), Vol. II.
[21] K. Otsuka, Phys. Rev. Lett. **65**, 329 (1990); Phys. Rev. A **43**, 618 (1991).
[22] T. Baer, J. Opt. Soc. Am. B **3**, 1175 (1986).
[23] L.M. Pecora, Phys. Rev. E **58**, 347 (1998).
[24] V.I. Arnold, *Geometrical Methods in the Theory of Ordinary Differential Equations* (Springer, Heidelberg, 1983).
[25] J. Guckenheimer and P. Holmes, *Nonlinear Oscillations, Dynamical Systems and Bifurcations of Vector Fields* (Springer, Heidelberg, 1983).
[26] J.D. Crawford, Rev. Mod. Phys. **63**, 991 (1991).
[27] T. Erneux and P. Mandel, Phys. Rev. A **52**, 4137 (1995).
[28] S.M. Baer and T. Erneux, SIAM (Soc. Ind. Appl. Math.) J. Appl. Math. **46**, 721 (1986); **46**, 1651 (1992).
[29] G. Kozyreff and P. Mandel, Phys. Rev. A (to be published).
[30] S. Nichols and K. Wiesenfeld, Phys. Rev. A **45**, 8430 (1992).
[31] S.H. Strogatz and R.E. Mirollo, Phys. Rev. E **47**, 220 (1993).